GENERATING SURFACES FOR REGISTRATION AND WARPING FE MESHES FOR THE FORWARD MODEL IN EIT OF BRAIN FUNCTION

A. Tizzard*, D.S. Holder** and R.H. Bayford***.

* Middlesex University/Product Design and Engineering, London, UK
** University College/Department of Medical Physics and Bioengineering, London, UK
***Middlesex University/School of Health and Social Sciences, London, UK

a.tizzard@mdx.ac.uk

Abstract: The research group at University College, London has been investigating the application of Electrical Impedance Tomography (EIT) to the diagnosis of epilepsy and stroke using finite element meshes based on realistic anatomical geometric models for the forward solution. The process of generating patient-specific meshes is highly labour intensive and so it is proposed that a standard mesh be warped such that it more closely matches that of the subject. This paper presents the initial stages of this process: a bi-cubic B-Spline patch is approximated through the electrode positions and then further refined by an iterative process such that it interpolates all of them to within 0.1 mm accuracy. Electrode and landmark positions are taken from eight human and one phantom tank model. For human subjects, the positions were digitised prior to routine EIT measurement and for the tank, from a CT dataset. Surfaces were successfully fitted to all subjects to the desired accuracy after a relatively few number of iterations. The method used to parameterise the electrode positions is discussed as well as how the initial surface approximation is made. Results show the accuracy of the surface when compared to that modelled from an actual subject.

Introduction

Electrical Impedance Tomography is a relatively new, non-invasive imaging method. It enables the internal electrical impedance of any object to be imaged by means of current injection and surface voltage measurements through an array of externally applied electrodes. The resulting aim therefore is to reconstruct images of conductivity changes within a body to assist in detection of any anomalies that may be identified from such a conductivity or impedance change. To obtain these images a sensitivity approach is utilised to reconstruct the conductivity distribution from a set of voltage measurements taken at the surface [1] [2] [3]. It employs a forward model and inverse solution based on the relationship:

$$\mathbf{v} = \mathbf{S}\boldsymbol{\sigma} \qquad (1)$$

Where $\mathbf{v}$ is the set of voltage measurements, $\boldsymbol{\sigma}$ is the conductivity distribution and $\mathbf{S}$ is the sensitivity matrix which can be considered as the Jacobian of the forward mapping (matrix of partial derivatives). The inverse solution generally used at present is a linearised approach which relates the conductivity change, $\Delta\boldsymbol{\sigma}$, to surface voltage change, $\Delta\mathbf{v}$ relative to a reference state by evaluating a pseudo-inverse of the matrix, $\mathbf{S}$. The use of realistic anatomy in the forward model used for image reconstruction in EIT of brain function appears to confer significant improvements compared to geometric shapes such as a sphere [4].

Accurate form may be achieved by geometrical models based on Magnetic Resonance Images (MRI) of the head, and this group has elected to use Finite Element Meshing (FEM) as it enables detailed internal anatomy to be modelled and has the capability to incorporate information about tissue anisotropy. The need for geometrically accurate FE meshes of the adult human head is now becoming more acknowledged and this group has already presented methods for their generation [5] [6] [7]. There is evidence to show in the aforementioned literature that the integrity of the FE model and its underlying geometry has significant and measurable effects on the quality of reconstructed images. At present, patient-specific meshes are generated by manually segmenting MRI datasets using a commercial surface modeller, the result of which is imported into a finite element software package for meshing. This process is highly labour intensive and time consuming and so would be inappropriate for time-critical clinical use, such as in EIT in acute stroke, when an image should be acquired and reported within 25 minutes. Therefore, it is proposed that a standard pre-existing realistic mesh of the human head be warped (morphed) such that it more closely matches that of the subject. It is still unclear as to what extent the geometric accuracy of the forward model affects image quality and localisation of impedance changes within the brain, though the results of recent work have shown that this could be significant [8]. It is clear, however, that FE meshes can be warped quite significantly with marginal effects on mesh integrity and image reconstruction quality when solved with a linear algorithm [9].

For rapid generation of FE meshes for specific patients within a time-critical clinical environment, a number of prior measurements of the subject need to be taken. To collect data for EIT imaging of brain function, the electrode arrangement is based on the EEG 10/20 configuration [10] [11]. In this investigation, the positions of these electrodes are used as the basis of the prior information in defining patient geometry. With such a methodology, only the area under the electrodes could undergo any non-rigid registration, though the remainder of the model may be shaped to a reasonable level of accuracy by affine transformation based on that registration. The mesh warping proposed in this work uses this hypothesis as a basis for generating patient-specific forward models. Additional data could easily be acquired by suitable design of the electrode cap or by some other means to include the positions of known registration points such as nasion, inion, and the left and right pre-auricular (periauricular) points. The nasion position can be quite accurately determined though the pre-auricular points and the inion positions are more subject to error owing to the variation of geometry in those regions between individuals. The use of electrode positions to redefine head surface geometry has been tried, for example [12] [13] [14]. This type of work is widely presented in the literature prompted largely by the need for reverse engineering of surface forms in design and manufacturing [15] [16] [17] [18]. The problem to be solved for this work is to construct a surface through a relatively small number (31) points that are already reasonably well-ordered.

This presentation outlines the methods used to define a bi-cubic B-Spline surface patch that interpolates all the electrode positions currently used for EIT of brain function, thereby defining a surface which matches that of the subject to within accuracy of 0.1 mm, or better, of the measured electrode positions. EIT electrode positions from nine subjects are taken; eight of these are human volunteers and patients under ethical approval. The ninth subject is a head-shaped phantom tank model containing a human skull and fixed electrode sites; the electrode and landmark positions were taken from a CT dataset of the model which was also use to generate a specific surface model for meshing [7].

Materials and Methods

For the human subjects, the electrode measurements were taken prior to routine EIT measurements using a *Microscribe* probe (www.immersion.com/digitizer/) with a manufacturer's reported positional resolution of 0.13 mm and accuracy of 0.38 mm. For the phantom model, the electrode positions were determined directly from the CT scan to within 1 mm accuracy.

The B-Spline method of interpolating curves and surfaces is a well established standard for geometric modelling in most modern Computer-Aided Design packages. The mathematical basis of the B-Spline is the subject of many texts in Computer Graphics and Computer-Aided Design, for example Foley & Van Dam [19], Onwubiko [20], Anand [21], mathworld (mathworld.wolfram.com/B-Spline.html) and many others. A B-Spline surface is defined by the tensor product:

$$C(u,v) = \sum_{i=1}^{m}\sum_{j=1}^{n} N_{i,k}(u) N_{j,l}(v) V_{i,j} \qquad (2)$$

where $C(u, v)$ is a point (x, y, z) on the resulting B-Spline surface, $V_{i,j}$ is a control vertex and $N_{i,k}(u)$ and $N_{j,l}(v)$ are B-Spline basis functions.

The electrode head-net used for EIT has been adapted from that used in EEG with additional electrode sites to make the number up to a total of 31 as depicted in Figure 1. The 10-20 positions are named such as to suggest a parameterisation of the electrode positions [11]. The additional electrodes standardized by the American Electroencephalographic Society occupy positions mid-way between the international 10-20 standard positions. Therefore a parametric grid of 10 by 10 spans is indicated, though the EIT arrangement does not include the landmarks comprising nasion, inion and pre-auricular positions as electrode sites and the four additional EIT specific sites will further modify the parameterisation. Removal of the landmarks from the parameterisation therefore indicates a grid of 8 by 8 spans or 9 by 9 points. If a B-spline surface is to fit through the electrode positions then some or all of them will need to lie on this regular, uniform and rectangular parametric grid.

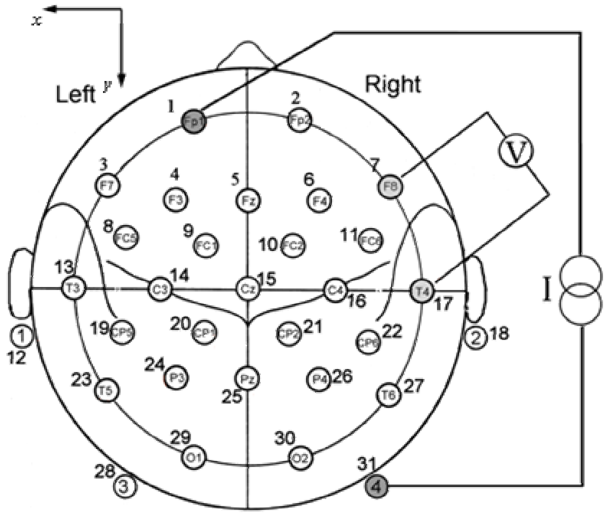

Figure 1: EIT electrode positions

The *Microscribe* probe was used to record the three-dimensional Cartesian position for the centre of each electrode on the scalp, prior to electrode insertion, as well as the nasion, inion and left and right periauricular points. Throughout the measurement process, it was essential that the subject underwent minimal movement in order to reduce measurement error. This is very difficult to achieve in practice and therefore constitutes the most significant source of error in the study. The origin position and axis orientation of the measurements were relatively arbitrary and so subsequent analysis was necessary to perform affine registration to a standard head mesh for which the positions of the four registration landmarks were known. A procedure was then established to align the electrode position measurements to the coordinate system as indicated in Figure 1 - that is right to left in the positive *x* direction, nasion to inion in the positive *y* direction with the head orientated upright in the positive *z* direction.

The boundary points from Figure 1 are clear; these being electrode numbers [1 2 7 17 18 31 30 29 28 12 13 3] working clockwise. The B-Spline surface, being quadrilateral in parameter space, needs to be a standard four-sided patch. The four sides can be defined, therefore, by the boundary electrode positions: [3 1 2 7], [7 17 18 31], [31 30 29 28] and [28 12 13 3]. These can be renamed to denote their parametric position on the surface patch as $\boldsymbol{u}_{0.0}$, $\boldsymbol{v}_{0.0}$, $\boldsymbol{u}_{1.0}$ and $\boldsymbol{v}_{1.0}$ respectively. The electrodes, if mounted correctly on a subject, are therefore uniformly spaced with sub-sets of electrodes lying on clearly identifiable curves. The directions of these curves are generally in the *x* and *y* directions which correspond to the parametric directions *u* and *v* respectively. In the *u* direction these are the boundary curves: $\boldsymbol{u}_{0.0}$ and $\boldsymbol{u}_{1.0}$ as well as five additional curves defined by electrodes: [3 4 5 6 7], [13 14 15 16 17], [12 23 24 25 26 27 18], [19 20 21 22] and [8 9 10 11]. The latter two curves do not intersect the boundary curves and need to be extended to points interpolated on those boundary curves. Also, the curve defined by [3 4 5 6 7] intersects the patch boundary at the corner making that particular spline non-isoparametric. However, a simplification of the surface patch boundary could be implemented; the lengths of the curves defined by electrodes [28 12 13 3] and [7 17 18 31] are equal whereas those defined by [3 1 2 7] and [31 30 29 28], i.e. $\boldsymbol{u}_{0.0}$ and $\boldsymbol{u}_{1.0}$, are not. The longer of the two latter curves is $\boldsymbol{u}_{0.0}$ and this can be truncated by interpolation either to match the length of $\boldsymbol{u}_{1.0}$ or to points defined by the parametric positions $u = {}^{1}/_{6}$ and $u = {}^{5}/_{6}$. This yields two more points to be considered in the surface patch boundary: 32 and 33, which will further modify the parameterisation indicated by the standards previously discussed. Thus $\boldsymbol{u}_{0.0}$ is now defined by points [33 2 1 32], $\boldsymbol{v}_{0.0}$ by [33 7 17 18 31] and $\boldsymbol{v}_{1.0}$ by [32 3 13 12 28]; $\boldsymbol{u}_{1.0}$ remains unchanged.

Thus the implication that the surface through the electrodes could be defined as a parametric grid of 8 by 8 spans could be drawn. This would generate a B-Spline control net of 9 by 9 vertices most of which would correspond to the approximate parametric positions of the electrodes. The exceptions would be that no electrodes or additional points would lie on the isoparametric curves v=0.125($\boldsymbol{u}_{0.125}$) and v=0.875 ($\boldsymbol{u}_{0.875}$); there would also be more significant mismatch between the control vertices where v=0.75 and the underlying electrodes defined by $\boldsymbol{u}_{0.75}$. A 9 by 9 B-Spline patch of this nature is relatively easy to generate from equation (2) which could be rewritten as:

$$\mathbf{C} = \mathbf{N}\mathbf{V}\mathbf{N}^{\mathrm{T}} \qquad (3)$$

as the B-Spline basis array, **N,** will be the same for both *u* and *v* for all subjects. In this case the edit points, **C**, are known and so the positions of the vertices on the control net, **V**, can be evaluated from:

$$\mathbf{V} = \mathbf{N}^{-1}\mathbf{C}\left(\mathbf{N}^{\mathrm{T}}\right)^{-1} \qquad (4)$$

Using the curves $\boldsymbol{u}_{0.25}$, $\boldsymbol{u}_{0.5}$ and $\boldsymbol{u}_{0.75}$ and the boundary curves $\boldsymbol{u}_{0.0}$, $\boldsymbol{v}_{0.0}$, $\boldsymbol{u}_{0.0}$ and $\boldsymbol{v}_{1.0}$ as an infrastructure a bi-cubic B-Spline patch can be defined using the following procedure:

1. Define the boundary curves $\boldsymbol{u}_{0.0}$, $\boldsymbol{u}_{1.0}$, $\boldsymbol{v}_{0.0}$ and $\boldsymbol{v}_{1.0}$ and truncate $\boldsymbol{u}_{0.0}$ either to the same length as $\boldsymbol{u}_{1.0}$ or by interpolating $u = {}^{1}/_{6}$ and $u = {}^{5}/_{6}$.
2. Define the quartile curves in the *u* direction $\boldsymbol{u}_{0.25}$, $\boldsymbol{u}_{0.5}$ and $\boldsymbol{u}_{0.75}$ to define the surface infrastructure using existing electrode points.
3. Interpolate nine equally spaced points on each of the curves in the *u* direction namely $\boldsymbol{u}_{0.0}$, $\boldsymbol{u}_{0.25}$, $\boldsymbol{u}_{0.5}$, $\boldsymbol{u}_{0.75}$ and $\boldsymbol{u}_{1.0}$ to define 35 additional points.
4. Generate B-Spline curves through these additional points in the *v* direction to generate 7 B-Spline curves.
5. Interpolate nine equally spaced points on each of these new curves and the boundary curves $\boldsymbol{v}_{0.0}$ and $\boldsymbol{v}_{1.0}$ to define a total of 81 edit-points to define the surface. These are arranged such that columns are points in the *v* direction and rows in the *u* direction.
6. Build the B-Spline basis matrix, **N**, with parameter spacing, 1/(*n*-1), where n is the number of edit points in each direction which, for this case, is nine.
7. Apply equation (4) to generate the control net, **V**.

The surface thus generated is an approximation of that which ideally fits through all the electrode positions. In order to achieve the best fit, the surface must be manipulated. The method to achieve this manually in commercial surface modelling software is to modify the position of the control vertices. In this case, an automatic method is presented that iteratively modifies the control net to minimise the distance of the electrodes from the surface. The first requirement for such automated surface manipulation is that the distance of each electrode from the B-Spline surface be known and this can be achieved by establishing the orthogonal projection of the point to the surface. This is a process covered by a number of authors as discussed by Hu and Wallner [22] who present the established first order method and also propose a second order algorithm. For simplicity, the first order algorithm is used.

A particular advantage of a B-Spline surface is its ability to provide local shape control within the vicinity of a control vertex. With this in mind, it is reasonable to predict that if a control vertex closest to an electrode with significant error is manipulated appropriately, the surface can be shaped to reduce the error to within a desired degree of accuracy. Considering the definition of the B-Spline surface in equation (2), and if the control net, V, was modified by ΔV such that $V_1 = V + \Delta V$ then a correspond change would take place in $C(u,v)$, that is:

$$\begin{aligned} C(u,v) + \Delta C(u,v) &= \sum_{i=1}^{m}\sum_{j=1}^{n} N_{i,k}(u)N_{j,l}(v)\left(V_{i,j} + \Delta V_{i,j}\right) \\ &= \sum_{i=1}^{m}\sum_{j=1}^{n} N_{i,k}(u)N_{j,l}(v)V_{i,j} \\ &\quad + \sum_{i=1}^{m}\sum_{j=1}^{n} N_{i,k}(u)N_{j,l}(v)\Delta V_{i,j} \end{aligned} \qquad (5)$$

and therefore:

$$\Delta C(u,v) = \sum_{i=1}^{m}\sum_{j=1}^{n} N_{i,k}(u)N_{j,l}(v)\Delta V_{i,j} \tag{6}$$

Relating this to equation (3) for a regular 9 by 9 grid, a positional change $\Delta V_{p,q}$ to a control vertex $V_{p,q}$ parametrically closest to an electrode off the surface at $C_{u,v}$ will result in a localised surface reshaping such that:

$$\Delta \mathbf{C}_{u,v} \approx \mathbf{N}_{p,p}\Delta \mathbf{V}_{p,q}\mathbf{N}_{q,q} \tag{7}$$

For a change in surface position at (u,v), the required change in the control vertex position is therefore given by:

$$\Delta \mathbf{V}_{p,q} \approx \frac{\Delta \mathbf{C}_{u,v}}{\mathbf{N}_{p,p}\mathbf{N}_{q,q}} \tag{8}$$

where p is the row and q the column of the 9 by 9 B-Spline basis array, **N**. While the shape control is localised, there will be minor, though possibly significant, changes to the surface form at other electrode positions within the immediate vicinity. Therefore a re-evaluation of the positional errors for all electrodes will need to take place and the shaping procedure reiterated; thus, the algorithm to iteratively manipulate the control vertices is as follows.

1. Generate a table of all electrodes off the surface by the desired positional accuracy and evaluate $\Delta \mathbf{C}_{u,v}$ for each.
2. For all such electrodes, establish the nearest control vertex, $\mathbf{V}_{p,q}$, to the electrode. For a surface defined by a grid of m by n points, the value p=round(u(n-1))+1 and q=round(v(m-1))+1. In the case currently considered here m=n=9.
3. For the same electrodes, evaluate $\Delta \mathbf{V}_{p,q}$ from equation (8).
4. Evaluate a new control vertex array as $\mathbf{V} = \mathbf{V} + \Delta\mathbf{V}$.
5. Repeat from step 1 until all electrodes are within the desired tolerance of the surface.

The initial approximation to the surface through the measured electrode positions for all nine subjects was implemented in a MATLAB (www.mathworks.com) routine taking the electrode positions, the surface degree, d (=3), and the number of edit points in each direction, n, as input variables to return a surface data structure. The surface manipulation procedure, defined by equations (7) and (8) was also implemented and applied to all subjects to achieve electrode positional tolerances of 0.1 mm and 0.05 mm to establish speed of convergence.

In order to evaluate the performance of the methodology described above, the surfaces generated through the electrodes need to be compared to the actual geometric form of the subject. This requires that a surface model of the subject, with which a comparison is made, needs to be built and meshed so that the deviation of the nodes on the surface of the Finite Element model from the surface through the electrodes can be established. No MRI datasets of usable quality were available for any of the human subjects used for the investigation described above, though the CT scan for the tank phantom provides a valuable source for making this comparison.

As previously stated, the electrode and landmark positions for the tank phantom were derived from the CT scan itself and the accuracy of the resulting positions was no better than 1 mm, this being the resolution of the CT image data. Moreover, the surface model generated from the dataset, [7], would suffer similar inaccuracies. Two tank meshes were used to evaluate the quality of the surface. These meshes consisted of 24722 elements and 52327 elements from which the boundary nodes were extracted and the orthogonal distances from those nodes and the B-Spline surface calculated. An acceptable result would be that a significant majority of the nodes be within 2 mm of the surface.

An even more accurate evaluation would result from aligning the surface more precisely with the mesh. As the accuracy of the landmark positions taken from the CT scan suffer the same inaccuracy of 1 mm, then it would be reasonable to assume that the surface could undergo affine linear transformation such that the distances of the nodes from the surface is minimised. In order to achieve this, a Newton-Raphson algorithm (secant method) was implemented that modified the position of the surface in relation to the meshes such that the sum of the distances, for x, y and z, was minimised. Again the distances from the nodes to the surface could be calculated. This procedure also results in providing an indication of inaccuracy in measuring the landmarks from the CT scan.

Results

A summary of results from the initial surface approximation, showing the errors between spline surfaces and electrodes which were greater than 0.1 mm, is given in Table 1. In addition, it lists the number of electrodes with the error and the electrode number with the maximum, e_{max}.

Table 1: Summary of positional errors > 0.1 mm for approximate surface for all subjects

subject	min	max	mean	STD	Count	e_{max}
1	0.116	2.811	0.890	0.980	10	8
2	0.119	3.480	2.079	1.225	9	21
3	0.111	6.340	2.074	2.196	9	10
4	0.209	3.178	1.763	0.964	10	9
5	0.153	3.418	1.657	1.007	10	10
6	0.102	2.914	1.385	0.821	10	9
7	0.665	4.554	2.423	1.391	8	22
8	0.269	4.165	1.632	1.515	8	10
9	0.181	4.103	1.458	1.109	11	19
mean	0.21	3.88	1.71			
Std	0.18	1.09	0.45			

The results of the surface manipulation procedure when applied to all subjects were as follows. To achieve an electrode to surface positional accuracy of 0.1 mm, the number of iterations ranged from 5 to 19 with the mean between 8 and 9 and a mode of 6. After manipulation of the control net, the maximum deviation of the electrode positions averaged 0.089 mm with a standard deviation of 0.007 mm. Halving the desired tolerance to 0.05 mm increased the number of iterations by an average of 20%, the range being between 6 and 24 with a mean of around 10 and mode of 8 iterations. The maximum deviation of the electrode positions from the final surface averaged 0.045 mm with a standard deviation of 0.005 mm.

A statistical analysis was carried out on the positional errors of the nodes directly under the surface from both meshes. For the 24722 element mesh, the mean positional error was 1.15 mm with a standard deviation of 0.87 mm, if the surface was not translated, and 1.03 ± 0.78 mm after minimising the sum of the errors in *x*, *y* and *z*. For the latter case, the overall positional translation of the surface was -0.36 mm, -1.06 mm, -0.57 mm in *x*, *y*, *z* respectively. For the denser mesh (52327 elements), these values were 1.18 ± 0.92 mm, not translated and 1.08 ± 0.86 mm when translated by -0.32 mm, -0.93 mm, -0.46 mm to minimise the sum of the errors. For both the translated surfaces, more than 88% of the nodes in the region considered were within 2 mm of the interpolated and manipulated surface. Figure 2 shows a typical statistical distribution of the nodal positional errors from the surface and a depiction of the surface fitted to the 24722 element mesh after translation.

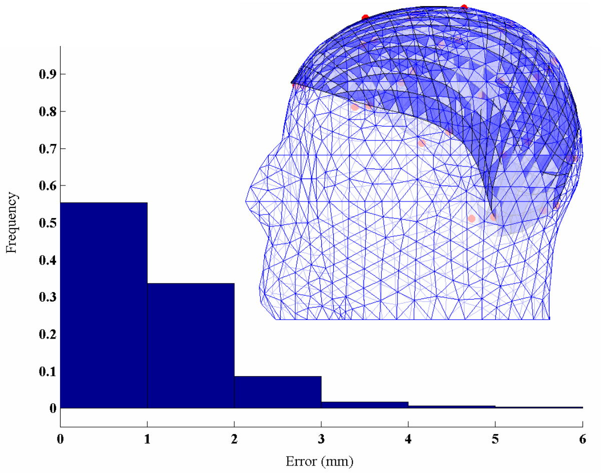

Figure 2: Typical statistical distribution of positional errors with final fitted surface.

Discussion

It has been demonstrated that a bi-cubic B-Spline patch, through measured electrode positions, can be approximated in the first instance, and then subsequently manipulated to achieve an accurate outcome. A relatively few number of iterations are required to manipulate individual control vertices such that positional errors between the electrode positions and the surface are reduced to as little as 0.1 mm. A relatively marginal increase in the number of iterations is required to halve this error value.

However, little value is gained from attempting to achieve too high a precision with the experimental data presented here. This is because electrode positions were obtained with an accuracy no better than 0.38 mm with the *Microscribe* device used. This value is the best case as further inaccuracies would have been incurred from subject movement during the measurement procedure. Furthermore, the landmark registration sites are also difficult to establish accurately, particularly the inion and pre-auricular points owing to variation in subject anatomy. Another, perhaps significant, source of error arises from the electrode placement itself. Though an experienced EEG technician can site electrodes with a reasonable level of consistency, there will still be an expectation that the parametric positions would be subject to errors that would be difficult to quantify. It is likely that the accumulation of these factors have had a bearing on the speed with which the surface manipulation algorithm converged as well as on the visual quality of the final surfaces generated.

Improvements to the surface generation are possible and would include engaging in the design of a more suitable head net and the use of Non-Uniform Rational B-Splines (NURBS). The latter is an extension of the B-Spline that applies weights to the control vertices to alter the locality of the control of surface form when manipulating a control vertex.

Conclusions

The results obtained from the analysis of the tank phantom surface and meshes are encouraging in that they show good conformity between a bi-cubic B-Spline surface fitted and manipulated through the measured electrode positions and surface nodes of the actual subject-specific finite element mesh. The latter surface model, being manually segmented from the CT scan of the tank phantom, will be subject to the normal errors associated with this type of modelling. The expectation that the maximum errors between the actual surface defined by the nodes of the FE model and that derived from electrode positions for this case would be in the region of 2 mm has been reasonably demonstrated.

In all cases presented, more than 80% of the nodes are within 2 mm of the surface and more that 94% are within 3 mm. Significant improvements in the measured accuracy are observed when the surface is translated to minimise the sum of the errors in *x*, *y* and *z*. There is a general conformity across the results regarding the amount translation the surfaces need to undergo in order to minimise the errors. The assertion that these values indicate the positional error in measuring the landmark and electrode positions from the CT scan is well supported by the data; the maximum movement in any one direction being in the region of the expected 1 mm predicted error.

Acknowledgements

These are due to Louise Enfield of University College, London, UK for providing the electrode position data for the human subjects used in this study.

ISSN: 1727-1983

References

[1] MURAI, T. and KAGAWA, Y. (1985): 'Electrical Impedance Computerised Tomography Based on a Finite Element Model', *IEEE Trans. Biomed. Eng.*, **32,** pp.177-84

[2] METHERALL, P., BARBER, D.C., SMALLWOOD, R.H., and BROWN, B.H. (1996): 'Three-dimensional electrical impedance tomography', *Nature*, **380,** pp.509-12

[3] GIBSON (2000): 'Electrical Impedance Tomography of Human Brain Function', PhD Thesis, University College London, UK

[4] BAGSHAW, A., LISTON, A.D., BAYFORD, R.H., TIZZARD, A., GIBSON, A., TIDSWELL, A.T., SPARKES, M.K., DEHGHANI, H., BINNIE, C.D., and HOLDER, D.S. (2003): 'Electrical impedance tomography of human brain function using reconstruction algorithms based on the finite element method', *Neuroimage*, **20,** pp.752-64

[5] BAYFORD, R.H., GIBSON, A., TIZZARD, A., TIDSWELL, T., and HOLDER, D.S. (2001): 'Solving the forward problem in electrical impedance tomography for the human head using IDEAS (integrated design engineering analysis software), a finite element modelling tool', *Physiol. Meas.*, **22,** pp.55-64

[6] BAYFORD, R.H., GIBSON, A., TIZZARD, A., LISTON, A.D., TIDSWELL, A.T., BAGSHAW, A., and HOLDER, D.S. (2001): 'Modelling the effect of eye sockets in the human head using I-DEAS and its implication for imaging impedance change using Electrical Impedance Tomography.', Proc. of XI International Conference on Electrical Bio-Impedance, Oslo, pp.391-96

[7] TIZZARD, A., HORESH, L., YERWORTH, R.J., HOLDER, D.S., and BAYFORD, R.H. (2005): 'Generating accurate finite element meshes for the forward model of the human head in EIT', *Physiol. Meas.*, **26,** p.S251-S261

[8] SOLEIMANI, M., ABASCAL, J.F.P.J., and LIONHEART, W.R.B. (2004): 'Simultaneous Reconstruction of the boundary shape and conductivity in 3d electrical impedance tomography', Proc. of XII International Conference on Electrical Bioimpedance and V Electrical Impedance Tomography, Gdansk, Poland, 2004, pp.475-78

[9] TIZZARD, A., BAYFORD, R.H., HORESH, L., YERWORTH, R.J., and HOLDER, D.S. (2004): 'Effects of Warping Finite-Elements Meshes for the Forward Model of the Head in EIT', Proc. of XII International Conference on Electrical Bioimpedance & V Electrical Impedance Tomography, Gdansk, Poland, 2004, pp.495-98

[10] BINNIE, C.D., ROWAN, A.J., and GUTTER, T. (1982): 'A Manual of Electroencephalographic Technology', (Cambridge University Press, Cambridge, UK)

[11] MALVIMUO, J. and PLONSEY, R. (1995): 'Bioelectromagnetism**:** Principles and Applications of Bioelectric and Biomagnetic Fields', (Oxford University Press, New York)

[12] GIBSON, A., RILEY, J., SCHWEIGER, M., HEBDEN, J., ARRIDGE, S., and DELPY, D. (2003): 'A method for generating patient-specific finite element meshes for head modelling', *Phys. Med. Biol.*, **48,** pp.481-95

[13] LAMM, C., WINDISCHBERGER, C., LEODOLTER, U., MOSER, E., and BAUER, H. (2001): 'Co-Registration of EEG and MRI Data Using Matching of Spline Interpolated and MRI-Segmented Reconstructions of the Scalp Surface', *Brain Topog.*, **14,** pp.93-100

[14] COHEN, F.S., IBRAHIM, W., and PINTAVIROOJ, C. (2000): 'Ordering and parameterizing scattered 3D data for B-spline surface approximation', *IEEE Trans. Pattern. Anal. Machine. Intelligence*, **22,** pp.642-48

[15] HOPPE (1994): 'Surface Reconstruction from Unorganized Points', PhD Thesis, University of Washington

[16] ECK, M. and HOPPE, H. (1996): 'Automatic Reconstruction of B-Spline Surfaces of Arbitrary Topological Type', Proc. of Annual Conference on Computer Graphics, New Orleans, LA, 1996, pp.325-34

[17] POTTMANN, H. and LEOPOLDSEDER, S. (2003): 'A concept for parametric surface fitting which avoids the parametrization problem', *Comput. Aided Geom. Design*, **20,** pp.343-62

[18] MAEKAWA, T. and KO, K.H. (2003): 'Surface construction by fitting unorganized curves', *Graphical Models*, **64,** pp.316-32

[19] FOLEY, J.D. and VAN DAM, A. (1982): 'Fundamentals of Interactive Computer Graphics', (Addison-Wesley, Reading, MA)

[20] ONWUBIKO, C. (1989): 'Foundations of Computer-Aided Design', (West, St Paul, MN)

[21] ANAND, V.B. (1993): 'Computer Graphics and Geometrical Modelling for Engineers', (John Wiley & Sons, New York)

[22] HU, S.-M. and WALLNER, J. (2005): 'A second order algorithm for orthogonal projection onto curves and surfaces', *Comput. Aided Geom. Design*, **22,** pp.241-60

ISSN: 1727-1983 © 2005 IFMBE